

Micro Beam Analysis of Interface in Advanced Materials Using Cs-Corrected STEM, ULV-SEM and FE-EPMA[†]

INOSE Akira^{*1} KITAHARA Yasuko^{*2} IKEMOTO Sachi^{*3} HASHIMOTO Satoshi^{*4}

Abstract:

The characteristic properties of advanced materials originate from interfacial or surface nanoscopic structures, and macroscopic structures are also controlled for their stable production. Various micro-beam analysis techniques, which cover the range from the atomic scale to the macroscopic scale, are required for detailed studies. Analyses using the spherical aberration corrected scanning transmission electron microscope (Cs-corrected STEM), ultra-low voltage scanning electron microscope (ULV-SEM) and field emission-electron probe microanalyzer (FE-EPMA) were used to characterize neodymium magnets, electronic materials such as power devices and noble metal fine particle catalysts. This paper presents the results of micro-beam analysis of these materials.

1. Introduction

Whether in structural materials or functional materials, control of microscopic surface structures, interfacial structures and others is critical for realizing the various physical properties of the materials concerned. Micro-beam analysis techniques such as electron microscopy, the surface analysis method and X-ray diffraction make it possible to analyze the microstructures of such materials^{1,2)}, and thus are critical techniques on par with chemical analysis, which enables highly accurate analysis of the average chemical composition of materials.

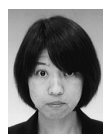
Responding to demand for high strength steel products, etc., the JFE Steel Group was the leader in introducing the spherical aberration (Cs) corrected scanning transmission electron microscope (Cs-corrected STEM), which enables analysis at the sub-angstrom level, the ultra-low voltage scanning electron microscope (ULV-SEM), which makes it possible to observe the top surface layer at the nanometer level, and other advanced technologies, and uses these instruments in nanoscopic structural analyses of iron and steel materials³⁻⁷⁾.

Based on these analytical techniques for iron and steel structures, JFE Techno-Research Corporation (JFE-TEC) was a pioneer in Japan to introduce leading-edge technologies (Cs-corrected STEM, ULV-SEM, FE-EPMA (field emission-electron probe micro-analyzer)), which support analysis at the nanometer scale, for various types of advanced functional materials that are now in the research and development process with the aim of realizing new properties, including neodymium magnets, materials for lithium ion secondary cells, noble metal catalysts and electronic materials. JFE-TEC proposes surface and interfacial structural analysis through appropriate specimen preparation and setting of analytical conditions for the material of interest, as well as analysis of the material data⁶⁻⁹⁾. Although high functions originate from nanoscopic structures, homogeneous formation of those structures at the macroscopic scale leads to stable development of properties. In other words, both structural analysis at the nanoscopic scale and correct

[†] Originally published in *JFE GIHO* No. 37 (Feb. 2016), p. 80–84



^{*1} Staff Manager,
Nano-scale Characterization Center,
Functional Materials Solution Div.,
JFE Techno-Research



^{*2} Staff Deputy General Manager,
Nano-scale Characterization Center,
Functional Materials Solution Div.,
JFE Techno-Research



^{*3} Staff Assistant Manager,
Nano-scale Characterization Center,
Functional Materials Solution Div.,
JFE Techno-Research



^{*4} Dr. Eng.,
Staff General Manager,
Tokyo Sales Office,
Sales Div.
JFE Techno-Research

evaluation of macroscopic average information are necessary.

As examples of this work, this report describes the results of structural analysis of neodymium magnets which manifest high coercivity as a result of control of the grain boundary structure at the nanometer (nm) level⁸⁾, multilayered structures at the level of several nm^{8,9)}, electronic materials in which electronic properties are changed by the interfacial structure⁷⁾ and noble metal fine particle catalysts with a size of several nm.

2. Structural Analysis of Functional Materials

2.1 Analysis of Grain Boundary Structure in Neodymium Magnets

The neodymium magnet is a type of permanent magnet that was invented in 1983 and is used in high efficiency motors in electric vehicles, air-conditioners, wind power generation, etc. In order to improve motor efficiency, microstructural control has been performed with the aim of increasing the coercivity of neodymium magnets^{11,12)}. For example, development of a technique for aligning single magnetic domain fine particles in the easy axis of magnetization has been developed¹¹⁾. The following presents examples of analysis of the metal microstructure and grain boundary structure in the millimeter macroscopic region to the nm order with commercial neodymium sintered magnets⁸⁾.

First, as an example of investigation of the elemental distribution and crystal orientation distribution over a wide region, **Fig. 1** shows the backscattered electron (BSE) images and elemental distribution in a neodymium magnet by FE-EPMA (JXA-8500F, manufactured by JEOL). Since the contrast of the BSE image in the high accelerating voltage region is caused by differences in the mean atomic number, the areas of uniform, somewhat dark contrast in the BSE image are considered to be the main phase ($\text{Nd}_2\text{Fe}_{14}\text{B}$ phase), the areas with the brightest contrast are considered to be an Nd-rich phase, and the areas of dark contrast is considered to be a B-rich phase. This could also be confirmed from the mapping results. Looking at the mapping results in Fig. 1 (a) in more detail, it can be understood that the main phase contains Dy and Pr concentration fluctuations, and the Dy and Pr have complementary distributions. Moreover, the results also reveal the existence of Pr and partial existence of Dy in the Nd-rich phase. The table in Fig. 1 (b) shows the results of a quantitative analysis of representative points by EPMA. Much of the Dy exists in the main phase, and its ratio is on the order of 1 at%. Although Nd, Dy, Pr and Fe and Mn have similar characteristic X-ray energies, it is possible to separate and analyze these elements by using a wavelength

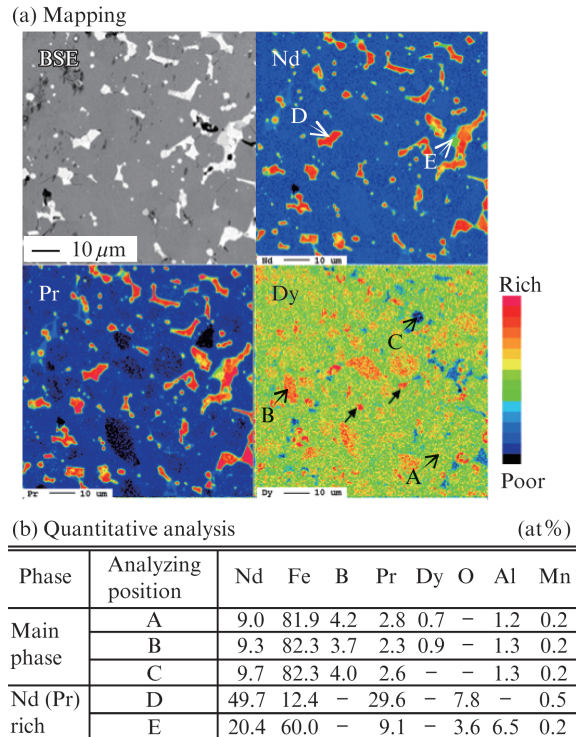


Fig. 1 FE-EPMA analysis of neodymium magnet

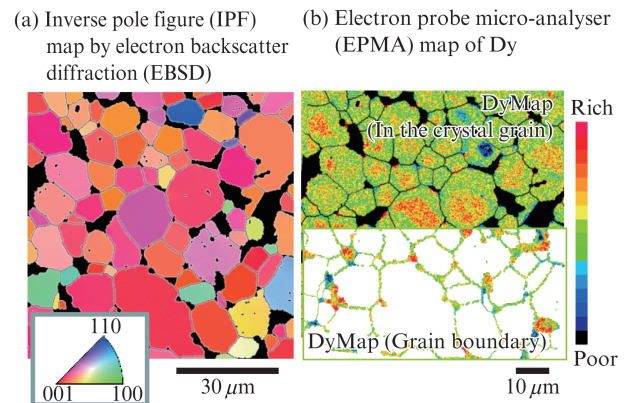
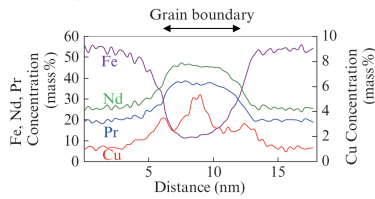


Fig. 2 Analysis of crystal orientation for neodymium magnet

dispersion type X-ray spectroscopy (WDX), which has high energy resolution.

Next, **Fig. 2** shows the result of an analysis of the orientations of important crystal grains for coercivity control of neodymium magnets with an electron backscatter diffraction instrument (EBSD) mounted in a SEM. Fig. 2 (a) is the inverse pole figure (IPF) map of the main phase ($\text{Nd}_2\text{Fe}_{14}\text{B}$: cubic crystal). Virtually all the crystal grains of the main phase show red to pink colors and have a [001] orientation. Fig. 2 (b) shows a map in which the EBSD crystal grain map (upper part) and grain boundary map (lower part) are superimposed on the elemental distribution of Dy obtained by EPMA. More detailed confirmation of the relationship between element segregation and grain boundaries is possible by measuring the same field of view. These results clarify

(b) Energy-dispersive X-ray spectroscopy (EDX) line analysis



(a) High-angle annular dark-field (HAADF) STEM image and atomic arrangement

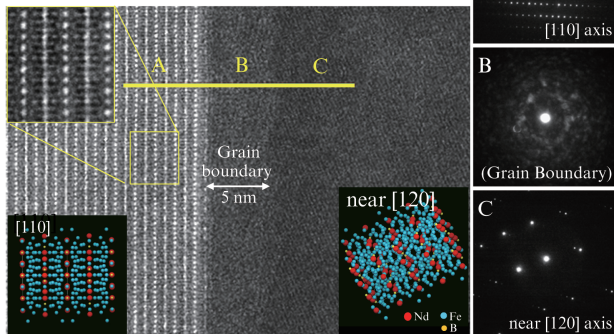


Fig. 3 Grain boundary of neodymium magnet analyzed by spherical aberration corrected scanning transmission electron microscope (Cs corrected STEM)⁷⁾

the fact that Dy is distributed near the center of the grains and at the triple point of the grain boundaries. Thus, quantitative evaluation of trace elements in a wide region is possible when FE-EPMA is used, and it is also possible to evaluate the correspondence of crystal orientation with elements by using EBSD in combination with FE-EPMA. Moreover, with EBSD, the easy axis of magnetization (C axis) with respect to the direction of magnetization (normal direction of the specimen) can also be investigated from the evaluation of the inclination of the respective grains.

Figure 3 shows an example of analysis of the structure of the crystal grain boundary structure in a neodymium magnet by using Cs-corrected STEM (JEM-ARM200F, manufactured by JEOL), which has atomic scale spatial resolution⁸⁾. Grain A in the high-angle annular dark-field scanning transmission electron microscope image (HAADF-STEM image) in Fig. 3 (a) has the [110] orientation. When compared with the structural model, it can be understood that the white dots correspond to atomic columns of Nd. The orientation of crystal grain C is close to [120], but the column is not clear because axial incidence was not performed. A grain boundary phase consisting of amorphous or microcrystalline materials with a thickness of approximately 5 nm exists at the grain boundaries. From the results of an EDX line analysis focusing on this grain boundary phase, it can be understood that a Nd- and Pr-rich grain boundary phase has formed, and Cu has concentrated at the interface between the Nd-rich grain boundary phase and the main phase. It has been shown that coercivity is

enhanced by the formation of this grain boundary phase^{10,12-14)}.

2.2 Analysis of Multilayer Thin-Film Interfaces in Electronic Materials

Use of SEM enables image observation and elemental analysis from millimeter scale macroscopic structures to nanoscopic structures. **Figure 4** shows the results of an analysis of the cross section of the wire bonding area in a semiconductor device with a ULV-SEM (ULTRA55, manufactured by Carl Zeiss AG)-EDX (NSS300, manufactured by Thermo Electron Co., Ltd.) under an accelerating voltage condition of 4 kV. The entire structure of the junction can be confirmed from the low magnification BSE image in Fig. 4 (a). The elemental mapping of the bonding area selected from the BSE image is shown in Fig. 4 (b). It can be understood that the intensity of Al and Au at the interface between the Al electrode and the Au wire is lower than in the bulk, and an alloy phase of AuAl with a thickness of approximately 200 nm has formed at the interface. Furthermore, the W layer, with a thickness of about 150 nm, could also be analyzed by separating Si and W, which have similar characteristic X-ray energies. Under the conventional high accelerating voltage condition, the spatial resolution of SEM-EDX was several μm , but JFE-TEC has clarified the fact that spatial resolution can be improved by more than two orders, to approximately 30 nm⁹⁾, by low accelerating voltage excitation¹⁵⁾.

Next, an example of observation of the superlattice of the compound semiconductor of an LED light-emitting device in which the arrangement is controlled at the atomic level will be presented. **Figure 5** shows the results of observation of the cross section of a GaAs/AlGaAs superlattice by Cs-corrected STEM⁸⁾. In the high resolution (HR) TEM image, an image corresponding to the transitional symmetry of the unit cell is obtained. In contrast to this, an image corresponding to

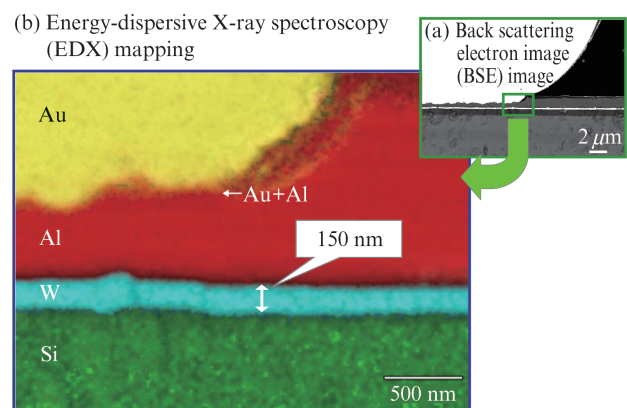


Fig. 4 Wire bonding area for semiconductor device analyzed using ultra-low accelerating voltage-scanning electron microscopy (ULV-SEM)

atom pairs of Ga-As and Al (Ga)-As is obtained in the HAADF-STEM image. In the low magnification image, the GaAs layers are observed as bright, and the AlGaAl layers, which have a low mean atomic number, are observed as dark. In the atomic resolution image, both atomic columns of the nearest atomic pairs of Ga-As, which have similar atomic numbers, have approximately the same intensity, whereas asymmetry of the intensity can be seen in the Al (Ga)-As. In many materials in which the manufacturing process is not controlled at the atomic level, there are cases where determination of the species of elements in ultra-small areas and information on chemical states is more important than the observation of atomic images. As an example, **Fig. 6** shows the results of EDX and EELS line analysis of a GaAs/AlGaAs superlattice by Cs-corrected STEM. Intensity is shown by the Ga K line in the EDX line profile and by the Ga L edge in the EELS line profile. Since a step interface was obtained in both profiles, spatial resolution was defined as the interface width to be 20–80% of EDX or EELS intensity. Resolution was approximately 1 nm,

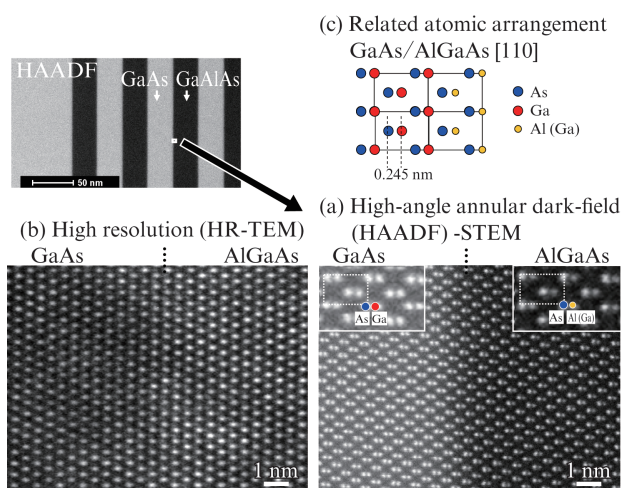


Fig. 5 GaAs/AlGaAs superlattice observed using spherical aberration corrected scanning transmission electron microscope (Cs corrected STEM)

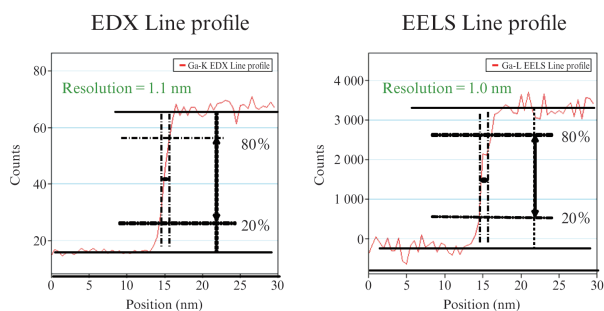


Fig. 6 Energy-dispersive X-ray spectroscopy (EDX) and electron energy-loss spectroscopy (EELS) line analysis of GaAs/AlGaAs superlattice using spherical aberration corrected scanning transmission electron microscope (Cs-corrected STEM) (Resolution is defined as interface width of 20–80%)

being 1.1 nm in EDX and 1.0 nm in EELS.

2.3 Analysis of Automotive Catalysts

In response to regulations on automobile exhaust gas accompanying increases in demand for automobiles with internal combustion engines, the development of automotive catalyst systems for detoxification of harmful substances has become an urgent issue¹⁶). Automotive catalysts consist mainly of supports, additives and noble metals. In particular, a noble metal with a size of the sub-nm to several 10 nm order is designed in a high dispersion. In many cases, the gas absorption method is used in evaluations of the particle size of noble metals¹⁷). However, for direct evaluation, a method which combines observation by electron microscopy and elemental analysis is effective. The following presents an example of observation of an automotive catalyst for gasoline-fueled automobiles. The Rh/CeO₂/Y₂O₃-ZrO₂ catalyst^{*}), which contains nanometer-sized Rh, was observed by Cs-corrected STEM^{*}). The catalyst sample was provided by Associate Professor Masaaki Haneda of Nagoya Institute of Technology.

Figure 7 shows the STEM images, FFT pattern obtained by FFT (Fast Fourier Transform) processing, and results of a qualitative analysis by EDX. Fig. 7 (a) is a low magnification bright field (BF) STEM image, in which only the support and the additives can be distinguished. Fig. 7 (b) shows the result of HAADF-STEM observation when the region enclosed in the square in that view is enlarged. At the edge of the half-moon shaped particle (arbitrary position: point 1), micro-particles (point 2) with a size of on the order of 1–2 nm can be observed at several places. When these were analyzed by EDX, it was found that point 1 is CeO₂ and point 2 is Rh, and an atomic arrangement can be seen in the Rh

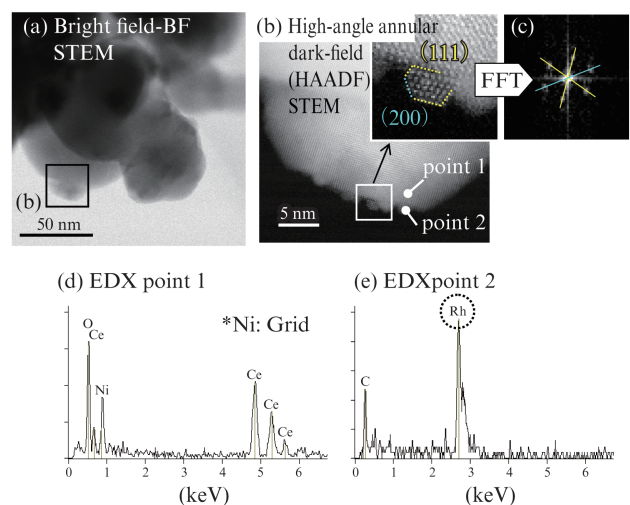


Fig. 7 Scanning transmission electron microscope (STEM) images, fast fourier transform (FFT) pattern, and electron energy-loss spectroscopy (EDX) spectra obtained from automotive catalyst

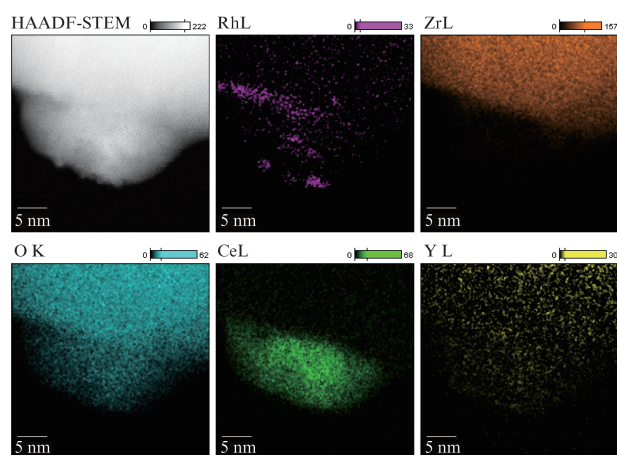


Fig. 8 Elemental mapping by energy-dispersive X-ray spectroscopy (EDX) and high-angle annular dark-field-scanning transmission electron microscope (HAADF-STEM) image

area, as shown in the enlarged view in the upper right corner of Fig. 7 (b). Based on this, it can be said that Rh has a crystalline structure. Moreover, from the results of the FFT analysis of the Rh particle area, it was found that (111) of Rh is in contact with the surface of the CeO_2 . **Figure 8** shows the results of STEM-EDX mapping of the area shown in Fig. 7 (b). In addition to Rh, which is supported by the CeO_2 surface, as mentioned above, it was possible to capture Rh distributed on the CeO_2 and at the $\text{ZrO}_2/\text{CeO}_2$ interface, which cannot be recognized from the STEM images.

3. Conclusion

The importance of micro-beam structural analysis from the nanoscopic scale to the macroscopic scale by utilizing Cs-corrected STEM, ULV-SEM and FE-EPMA was shown through examples of interfacial and structural analysis of high performance functional materials, including analysis of the grain boundaries in high coercivity neodymium magnets, the superlattice structure of compound semiconductors and a noble metal fine parti-

cle catalyst. JFE-TEC has accumulated a wealth of know-how, beginning with specimen preparation techniques optimized for each of these materials. In the future, the company will continue to introduce and develop, on a timely basis, the nanometer-scale micro-beam analysis techniques (i. e., specimen preparation, instruments, data analysis) necessary for clients who intend to develop new structural materials and/or functional materials, and will provide the results as the client's "Best partner for *monozukuri*."

References

- 1) Sato, K. 219–220th Nishiyama Memorial Seminar, ISIJ. 2014, p. 1.
- 2) Nagoshi, M. 219–220th Nishiyama Memorial Seminar, ISIJ. 2014, p. 161.
- 3) Funakawa, Y.; Shiozaki, T.; Tomita, K.; Yamada, K.; Maeda, E. ISIJ Int. 2004, vol. 44, p. 1945.
- 4) Hamada, E.; Yamada, K.; Nagoshi, M.; Makiishi, N.; Sato, K.; Ishii, T.; Fukuda, K.; Ujiro, T. Corr. Sci. 2010, vol. 52, p. 3851.
- 5) Nagoshi, M.; Kawano, S.; Sato, K. J. Surf. Finish. Soc. Jpn. 2003, vol. 54, p. 31.
- 6) Hashimoto, S. The journal of REAJ. 2006, vol. 28, p. 155.
- 7) Hashimoto, S.; Ogata, K.; Ikemoto, S.; Kitahara, Y.; Inose, A.; Maeda, C. Proceedings of the 30th annual meeting of The Rare Earth Society of Japan. 2013.
- 8) Sakurada, T.; Hashimoto, S.; Tsuchiya, Y.; Tachibana, S.; Suzuki, M.; Shimizu, K. J. Surf. Anal. 2005, vol. 12, p. 118.
- 9) Inose, A.; Hashimoto, S.; Ogata, K.; Maeda, C.; Yano, Y. SiC and a related semiconductor research 22nd time lecture manuscript collection. 2013.
- 10) Ohashi, K.; Omori, K.; Okabe, T.; Kobayashi, K.; Chikada, S.; Sagawa, M.; Sugimoto, S.; Tokunaga, M.; Hamano, M.; Hiro-sawa, S.; Hono, K. "Neodymium jisyaku no subete." Agne Gijyutsu Center, 2011, p. 101.
- 11) Tawara, Y.; Ohashi, K. "Kidorui Eikyu Jisyaku." Morikita Publishing, 2005, p. 92.
- 12) Hono, K.; Ohkubo, T.; Sepehri-Amin, H. J. Japan Inst. Met. Mater. 2012, vol. 76, p. 2.
- 13) Mishima, C.; Noguchi, K.; Yamazaki, M.; Matsuoka, H.; Mitarai, H.; Honkura, Y.; J. Japan Inst. Met. Mater. 2012, vol. 76, p. 89.
- 14) Itakura, M.; Kuwano, N. J. Japan Inst. Met. Mater. 2012, vol. 76, p. 17.
- 15) Hashimoto, S.; Sakurada, T.; Suzuki, M. J. Surf. Anal. 2008, vol. 14, p. 428.
- 16) e. g. Johokiko. "Jidousya Syokubai no Saishin Gijyutsu oyobi Rekka Taisaku to Kikinzoku Teigen." 2010, p. 75.
- 17) Kamiuchi, N.; Haneda, M.; Ozawa, M. Catalysis Today. 2013, vol. 201, p. 79.